How Different Wind Stress Patterns Affect the Tropical–Subtropical Circulations of the Upper Ocean

ZHENGYU LIU

UCAR Visiting Scientist Program, Program in Atmospheric and Oceanic Sciences, Princeton University, Princeton, New Jersey

S. G. H. PHILANDER

Program in Atmospheric and Oceanic Sciences, Princeton University, Princeton, New Jersey

(Manuscript received 5 March 1993, in final form 7 December 1993)

ABSTRACT

An oceanic GCM is used to investigate the response of the tropical and subtropical thermocline circulation and structure to different wind stress patterns. Although the subtropical winds do not affect the transport or the speed of the Equatorial Undercurrent significantly, they do change the equatorial temperature field in the lower part of the equatorial thermocline significantly. A weaker subtropical wind curl causes a cooling of the subsurface equatorial region and, hence, an intensification of the equatorial thermocline. A weakening of the subtropical wind curl by a factor of 2 cools the equatorial lower thermocline water by 2°C.

1. Introduction

Observations give clear evidence of an exchange of mass between the subtropical and the equatorial oceans (Tsuchiya 1981; Tsuchiya et al. 1989; Fine et al. 1981; Fine 1987; Toggweiler et al. 1989). Recent numerical and theoretical analyses confirm the close connection between the subtropical and the equatorial thermocline circulation (McCreary and Yu 1992; McCreary and Lu 1994; Liu et al. 1994; Liu 1994). For example, in a GCM study, Liu et al. (1994) found that about 2/3 of the water of the Equatorial Undercurrent (EUC) in the western part of a basin comes from the eastern part of the subtropical gyre. Liu (1994) uses a simple ventilated thermocline model to examine the physical mechanisms that determine the water exchange between the Tropics and subtropics. One purpose of this paper is to test Liu's (1994) results with GCM experiments. In addition, we investigate the response of the tropical circulation and temperature field to subtropical winds.

First, we investigate to what extent changes in the subtropical winds affect the EUC. Liu (1994) finds that the equatorward mass flux is mainly determined by the tropical easterly wind at the southern boundary of the subtropical gyre rather than by the winds over the subtropical gyre. A stronger subtropical wind curl only produces an enhanced recirculation within the subtropical gyre. Hence, one may speculate that the EUC transport will not be changed by the subtropical wind significantly. This inference needs to be confirmed.

Next, we turn to the equatorial thermocline structure. The insensitivity of the EUC to subtropical winds could lead one to conclude that the equatorial temperature field is not affected by the subtropical wind either. Our calculations indicate otherwise: the subtropical wind does change the tropical temperature field significantly.

This paper is arranged as follows. The model and the experiments will be introduced in section 2. In section 3, we discuss the connection between the tropical and subtropical circulation from integrated transport fields. Section 4 focuses on the response of the equatorial circulation, particularly the EUC, to various subtropical and tropical wind forcing. Section 5 reports the response of equatorial thermocline to various wind forcing. A summary and further discussion are given in section 6. Some details about the spinup process of the subtropical–tropical temperature field will also be given in the appendix.

2. The model and the experiments

a. The model

The finite differencing is the same as Bryan (1969) as implemented in the GFDL MOM 1.0 code (Pacanowski et al. 1991). The domain is an idealized rectangular basin from 40°S to 40°N in latitude and from 0° to 60° in longitude, with a flat bottom at 3000 m.

Corresponding author address: Dr. Zhengyu Liu, Department of Atmospheric and Oceanic Sciences, University of Wisconsin–Madison, 1225 W. Dayton Street, Madison, WI 53706.

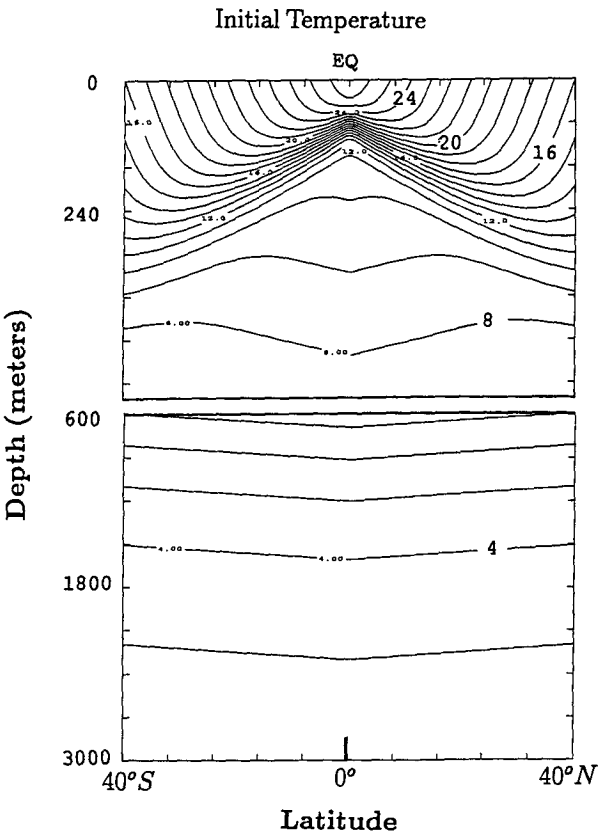

FIG. 1. The initial zonally independent temperature field for runs A–E. The surface and boundary temperatures are also used as restoring temperatures on the surface and domain boundaries.

The longitude resolution is 1°; the latitudinal resolution is 1/3° within 6° of the equator and increases linearly to 1° at the domain boundaries on 40°. There are 30 levels in the vertical with a 10-m resolution in the top 100 m.

Horizontal mixing is the constant coefficient scheme with the eddy viscosity and diffusivity of 2×10^7 and 10^7 cm^2 s^{-1}, respectively. Two sponge layers are added poleward of 35°, in which temperature is restored to prescribed values with a restoring time of 40 days at 35° decreasing to 4 days at 40°, while the eddy viscosity for momentum equations is increased linearly to 2×10^8 cm^2 s^{-1} from 35° to 40°. In the vertical, a Richardson number–dependent scheme is used (Pacanowski and Philander 1981), with a background viscosity and diffusivity of 1 and 0.1 cm^2 s^{-1}, respectively. Unstable temperature gradients are eliminated by mixing heat vertically to a depth that ensures a stable density gradient.

The initial condition is a state of rest. Salinity is taken as a constant of 35 psu. The initial temperature is prescribed to be zonally independent and symmetric about the equator, as shown in Fig. 1. This initial latitudinal temperature profile at the surface is also used to restore the surface temperature during all the experiments with a 40-day relaxation time. Poleward of 35° this temperature profile is also used to restore temperatures in the sponge layers.

b. *The experiments*

Results from six experiments will be discussed. In all the experiments, the forcing and initial conditions are symmetric about the equator. The experiments are summarized in Table 1. They differ from each other in the wind stress, as plotted in Fig. 2. In the control run, run A, the wind stress (Fig. 2a) consists of two parts: a uniform easterly wind within 12° of the equator and a subtropical wind between 12° and 35° with a negative wind curl.

In runs B, C, and D, the wind stress of the control run is perturbed. In run B, the wind curl in the subtropics is reduced by a half (Fig. 2b). In contrast, in run C, the tropical easterly wind is reduced by a half (Fig. 2c). Run D is a reduction of the wind by a half everywhere (in both magnitude and vorticity), corresponding to a combination of runs B and C (Fig. 2d).

In two additional cases, the wind profiles are changed drastically and unrealistically. In run E, a "uniform" (or no curl) easterly wind occupies the entire domain (Fig. 2e). (Notice the spherical factor: the wind is actually not exactly constant.) In run F, the easterly wind is suppressed within 5° of the equator and the rest of

TABLE 1. Experiments and transports (in Sv) of barotropic gyres, meridional cells, and the EUC whose maximum EUC speed is in centimeters per second. The letter "N" stands for "does not exist." The transport of equatorial cell and subtropical cell is observed from the meridional transport streamfunction (Fig. 3), with the former as the streamlines within 5° and the latter outside 5°.

		Gyre			Cell	
Experiment	Wind feature	Subtropical	Equatorial	EUC (max$U$)	Equatorial	Subtropical
A	Control	32	6.3	16.5 (68)	25	8
B	Half-subtropical wind	16	5.8	14.5 (74)	23	7.5
C	Half-easterly wind	32	2.2	8.9 (50)	6	6.5
D	Half-wind	16	2.1	7.8 (52)	5	6
E	All-easterly	N	5.3	12.8 (78)	22	7
F	No-easterly	34	N	2.0 (7)	N	N

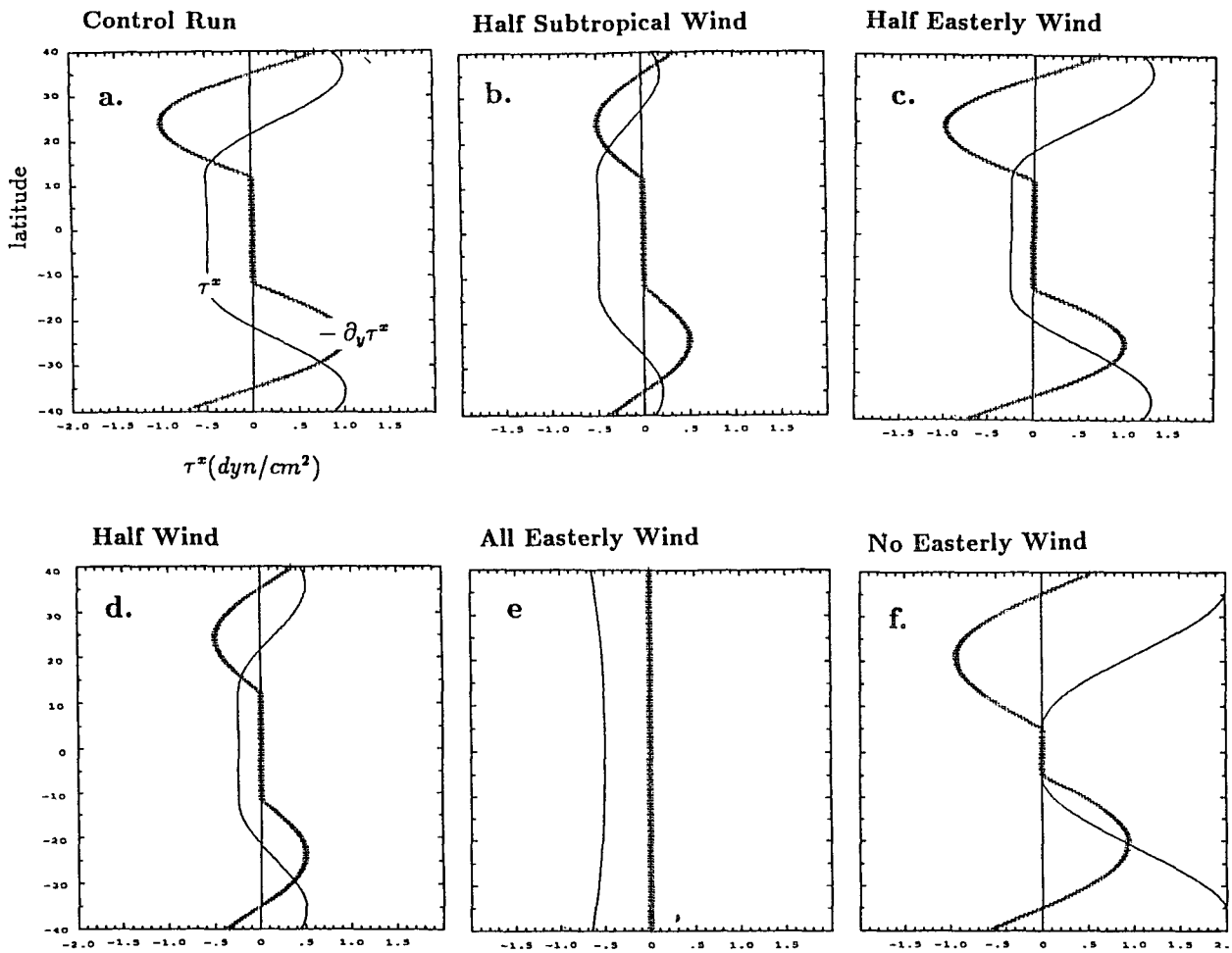

FIG. 2. The zonal wind stress and vorticity (arbitrary unit but the same for all the runs) for the six runs: (a) control run, (b) half-subtropical run, (c) half-easterly run, (d) half-wind run, (e) all-easterly run, and (f) no-easterly run.

the ocean surface is forced by westerly winds with a curl comparable to that of control run (Fig. 2f).

Except for run F, the model is integrated for 17 years. At that time the temperature still exhibits a slow trend, which is presumably due to the deep thermohaline spinup process. However, long before that time, in both the equatorial and subtropical regions, the thermocline temperature field has reached quasi-equilibrium evolution; that is, the temperature equation the local variability is negligible (see the appendix). The integration is long enough to capture the dynamical features of the steady thermocline and the circulation of the subtropical–tropical ocean system. Run F starts from the control run at year 13 and continues for another 7 years. All of the analyses in the paper use the time mean of the last year in each experiment.

3. The subtropical–tropical mass exchange

Liu et al. (1994) discuss in detail the subtropical–tropical mass exchange in the control run. Liu (1994) describes the physical mechanism that controls the exchange. Here, we discuss only the integrated mass exchange field in different GCM experiments.

a. Streamfunction field

The pattern of the vertically integrated streamfunctions (not shown) consists of subtropical gyres and equatorial gyres. The subtropical pattern resembles that of Munk's circulation, which has a viscous western boundary layer. As predicted by Sverdrup theory, the gyre transport increases linearly with wind curl (Table 1). In the all-easterly run (run E), however, there is no barotropic circulation in the extratropics due to the lack of wind curl.

Within 5° of the equator, the "uniform" easterly wind (except for run F) forces two counterrotating barotropic equatorial gyres, with the eastward flow within 2° of the equator. This equatorial gyre is caused by the nonlinearity associated with the EUC (Philander and Pacanowski 1980). The transport of an equatorial

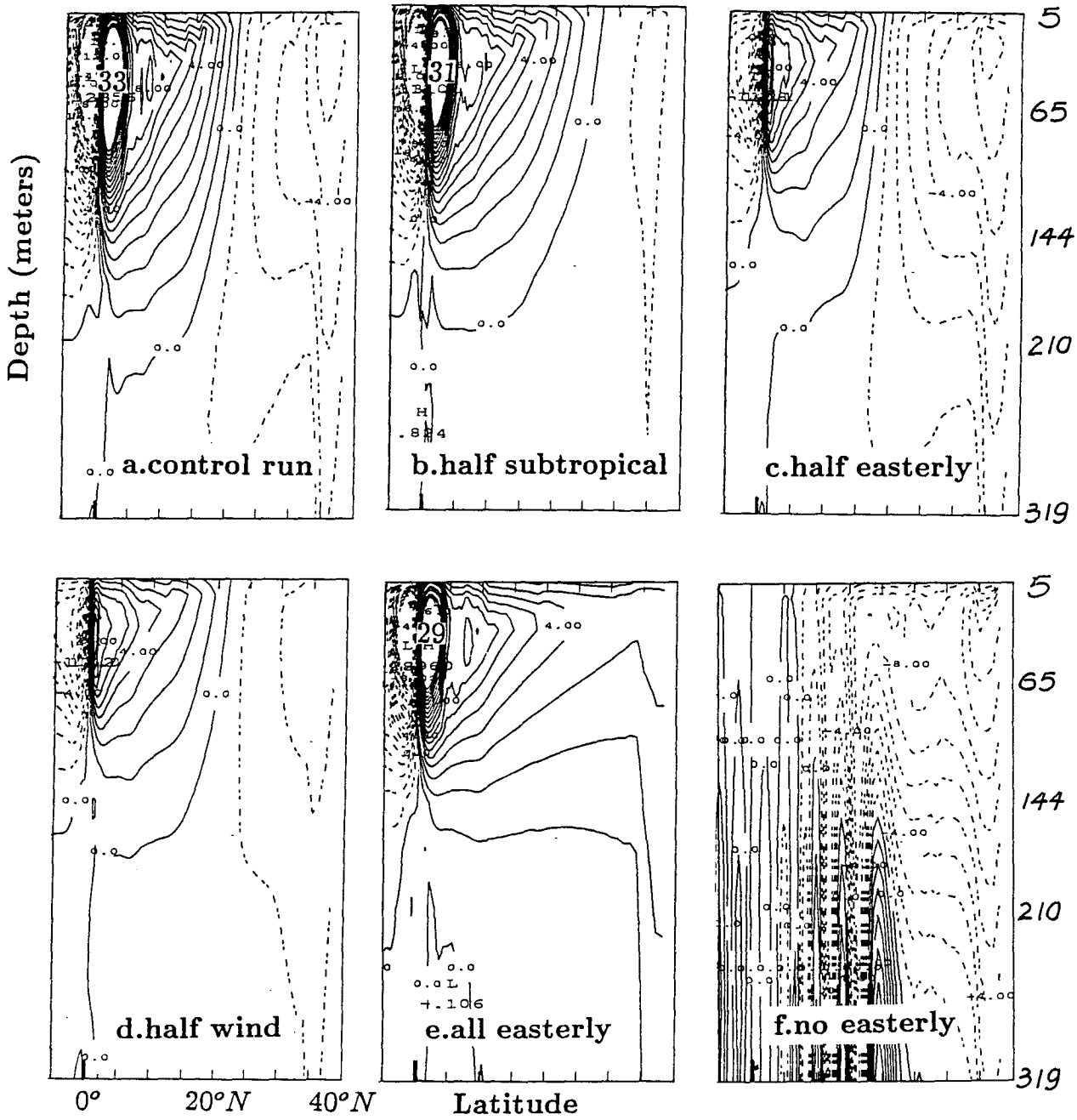

FIG. 3. Meridional streamfunctions for (a) the control run, (b) the half-subtropical run, (c) the half-easterly run, (d) the half-wind run, (e) the all-easterly run, and (c) the no-easterly run. The contour interval is 1 Sv. Contour values beyond ±20 Sv are not drawn.

gyre in each run is presented in Table 1. In the control run, the transport is about 6.3 Sv. When the subtropical wind curl is reduced by a half (half-subtropical run) or even vanishes (the all-easterly run), the transport of the equatorial gyre reduces only slightly. Thus, the equatorial gyre is not affected by the subtropical wind. If, however, the local easterly wind is reduced by a half (half-easterly run and half-wind run), the transport is reduced by about 60%. When the equatorial easterly vanishes (no-easterly run), the equatorial gyre disappears.

Between the subtropical gyre and the equatorial gyre, there is no barotropic flow at all, because of the absence of wind curl. As discussed by Liu et al. (1994), the water exchange occurs mainly in the meridional plane. Thus, we turn to the meridional streamfunction field.

Figure 3a shows the zonally integrated streamfunction for the control run. In one subtropical–tropical

system, there are two meridional circulation cells in the upper ocean. (Hereafter, we will use "cell" to refer to zonally integrated meridional circulation, and "gyre" for vertically integrated horizontal circulation.) In the upper 120 m and within 5° of the equator is the intense equatorial cell with a transport of 33 − 8 = 25 Sv (Sv ≡ 10^6 m^3 s^{-1}). Outside the equatorial cell is a much broader and slower subtropical cell (McCreary and Lu 1994), which contributes significantly to the mass exchange between the subtropical and equatorial regions (Liu et al. 1994).[1]

In the three perturbation runs (runs B, C, and D in Figs. 3b,c,d), the meridional cells are qualitatively similar to that in Fig. 3a. Quantitative changes are summarized in Table 1. With half the subtropical wind curl (run B, Fig. 3b), both the equatorial cell and the subtropical cell decrease only slightly (less than 1 Sv). If the tropical easterly is reduced by a half (run C, Fig. 3c), surprisingly, the equatorial cell reduces dramatically by more than three-fourths, while the reduction of the subtropical cell is less than 3 Sv (less than half of the transport of this cell). If the wind is reduced by a half everywhere (Fig. 3d), the result is like the combination of runs B and C.

When a uniform easterly prevails everywhere (run E, Fig. 3e), the subtropical cell extends deeper into the extratropics and the equatorward return flow tends to shoal. When the easterly wind is absent (run F, Fig. 3f), the subtropical cell disappears.

These experiments confirm that the existence of the equatorial cell and subtropical cell is mainly determined by the tropical easterlies. The subtropical wind changes both cells only slightly (less than 1 Sv). The strength of both the equatorial and easterly subtropical cells depends nonlinearly on the tropical easterly. The former decreases faster than the wind while the latter decreases more slowly than the wind. The strength of these cells is therefore not determined only by the strength of the surface Ekman transport, which varies linearly with the wind. In addition, as discussed before, the transport of the equatorial gyre also seems to decrease faster than the wind, although not as fast as the equatorial cell. The nonlinearity of the equatorial dynamics [see the momentum balance in (A.1)] seems to be consistent with the nonlinear dependence of the equatorial gyre and equatorial cell on the wind.

b. Subtropical–equatorial mass exchange

Figure 4 shows the total poleward and equatorward transports within the upper 320 m for the various experiments. Positive curves represent northward transport and negative curves southward transport. The total northward (or southward) transport, the transport within the western boundary current, and the Ekman transport are represented by solid lines, dash–dotted lines, and heavily dotted lines, respectively. The control run (Fig. 4a) and the three perturbation runs (runs B, C, D in Fig. 4b,c,d) are qualitatively similar. First, the transport through the western boundary is dominant only in the subtropical gyre. Second, the total northward and southward transport tend to compensate in the upper 320 m (solid lines). They are characterized by two maxima: one corresponds to the subtropical gyre and the other to the equatorial cell and equatorial gyre. Between the two maxima is the minimum, representing the subtropical–equatorial mass exchange. Its transport is less than the Ekman transport by 1–3 Sv because of the surface southward geostrophic flow (for details, see Liu et al. 1994).

A reduction in the subtropical wind curl by a half (Fig. 4b) reduces the maximum subtropical transport linearly by a half, as expected from Sverdrup theory. However, the maximum transport decreases only slightly (3 Sv) in the equatorial region. The minimum transport at 12° remains almost the same as in the control run. In contrast, if the easterly is reduced by a half (Fig. 4c), the transport remains unchanged in the subtropics but is reduced dramatically, by more than a half, in the equatorial region. As seen before, this reduction comes mainly from the reduction of the equatorial cell (by about 3/4) (see Table 1). The minimum transport at 12° decreases by about 4 Sv, about the reduction of the local Ekman transport. When the wind is reduced by a half everywhere (Fig. 4d), the reduction is about the combination of the those in Fig. 4b and Fig. 4c. Figures 4a–d confirm that it is the tropical easterly wind that determines the exchange transport. This impression is reinforced by the two extreme runs. Figure 4e shows that even in the absence of the subtropical wind curl, the exchange transport remains similar to that in the control run. In contrast, Fig. 4f shows only a tiny exchange transport, of less than 2 Sv, in the absence of easterly winds.

The GCM results support the theoretical results of Liu (1994): the exchange transport is determined mainly by the tropical winds rather than by the subtropical winds. Furthermore, the reduction of the exchange transport with respect to Ekman transport stays within the range of about 15%–30% in the various experiments. Physically, the wind forcing in these experiments is strong enough for the ventilated zone to extend into the equatorial region. In this regime of wind forcing, the reduction of the Ekman transport in the surface layer is not sensitive to the wind forcing (Liu 1994).

Finally, a closer look at Fig. 4 shows that the subtropical wind curl has a small effect on the exchange transport. A stronger subtropical wind tends to increase the exchange transport by about 1 Sv in all the cases. The subtropical wind also influences the equatorward

[1] Farther poleward adjacent to the subtropical cell is the westerly subtropical cell, with sinking on the equatorial side and upwelling on the polar side. This cell contributes little to the subtropical–tropical mass exchange. Thus, this cell will not be studied here.

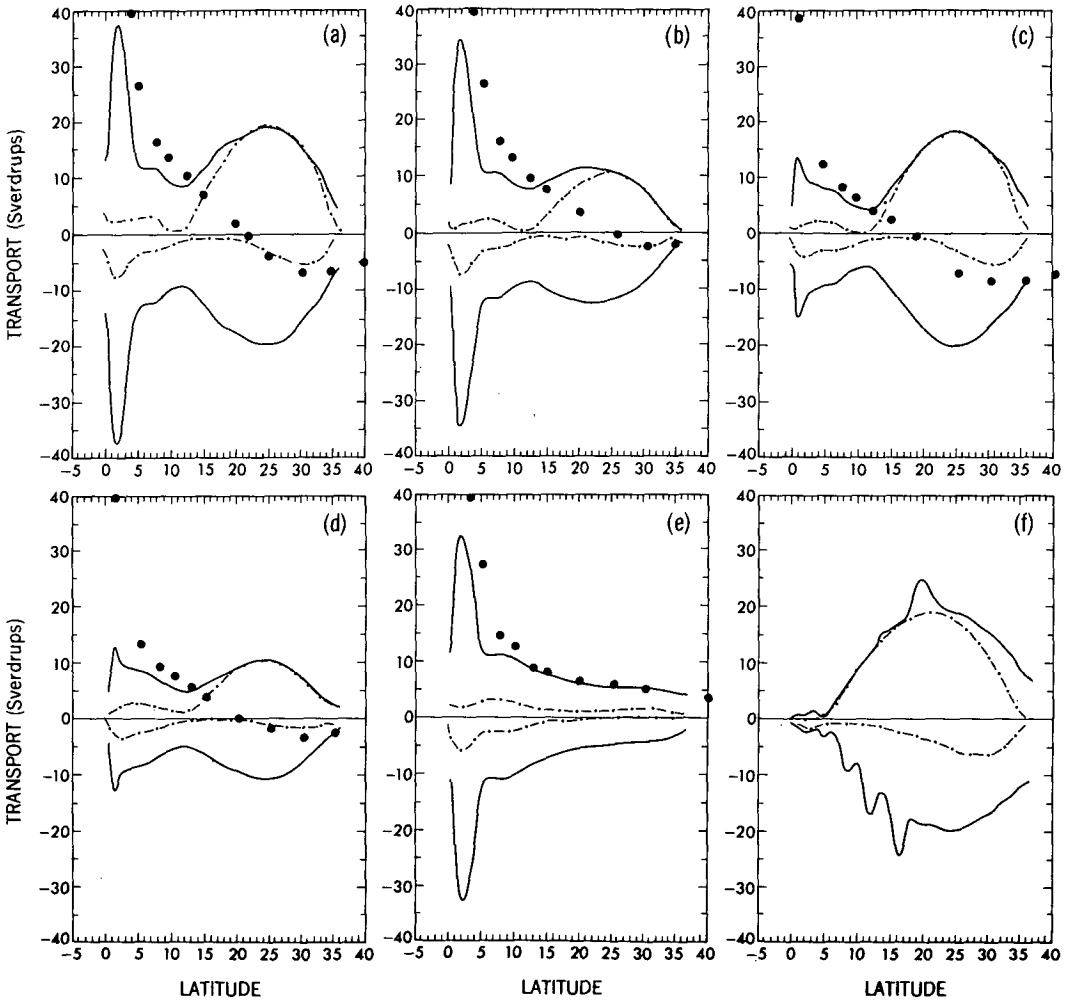

FIG. 4. The total northward (positive) and southward (negative) meridional transport (solid lines) for each run in the upper 320 m. The total western boundary northward and southward transports (within 5° longitude of the western boundary) are drawn as dash–dotted lines. The heavy dots in (a)–(e) represent the Ekman transport.

low latitude western boundary current (the negative maximum at 2°N in the dash–dot lines). A comparison of the all-easterly run with the control run in the Tropics shows a reduction of the low–latitude western boundary transport by about 2 Sv. Moreover, in the case with no winds near the equator, the small equatorward exchange transport (2 Sv) is accomplished by the low latitude western boundary current.

Since the transport of the low-latitude western boundary is crucial to the initial EUC transport (near the western boundary) (Liu et al. 1994), one may expect the subtropical wind to affect the initial EUC transport, although not strongly. However, the maximum EUC transport will hardly be changed.

4. Equatorial circulation under various winds

The above GCM results confirm that the exchange transport is mainly determined by the tropical easterly wind, as speculated by Liu (1994). Since the exchange transport contributes to more than half of the EUC transport (Liu et al. 1994), one may expect that the EUC transport is determined mainly by the tropical easterly.

The magnitude of zonal velocity in the equatorial plane is depicted in Fig. 5 for the six runs. The control run (Fig. 5a) shows a westward surface flow in the top 20 m and a subsurface EUC with a maximum of 68 cm s^{-1}. The core of the EUC is deepest near the western boundary at 250 m and is at 150 m near the eastern boundary. Along a meridional section (not shown), the EUC is confined within 2° of the equator and is surrounded by westward wind-driven flow on the top and on both sides. Below the EUC is a weak westward flow. All these structures agree well with previous GCM experiments and observations.

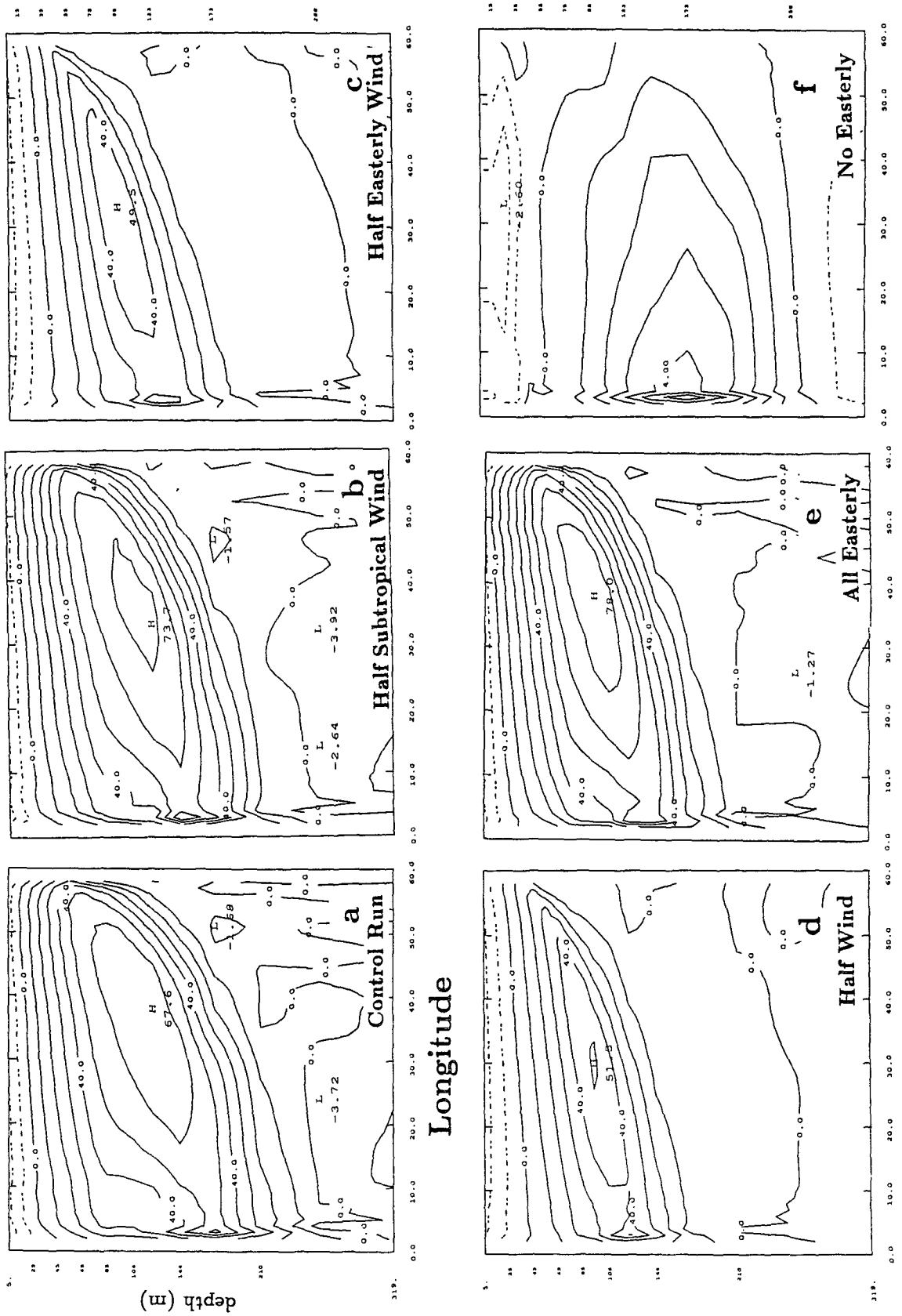

FIG. 5. The zonal velocity values along the equatorial plane for each run. Contour interval: 10 cm s^{-1} in (a)–(e). Contour interval: 1 cm s^{-1} in (f).

The maximum transports and speeds of the EUC in the various runs are listed in Table 1. Figure 6 shows longitudinal variations in the EUC transports. They are calculated as the eastward transport of the upper 300 m within 5° of the equator. For the control run (curve a), the maximum transport of 17 Sv is reached in the midbasin. The transport increases rapidly near the western boundary but decreases slowly in the interior (and then decreases rapidly again within 10° of the eastern boundary).

When the subtropical wind curl is reduced by a half (Fig. 5b), the equatorial circulation hardly changes. The maximum EUC speed is even slightly larger than in the control run. But the undercurrent is slightly shallower in the western basin. As a result, the total transport is less than that of the control run by about 1 Sv, as shown in Fig. 6 (curve b). When the easterly wind is reduced by a half, the magnitude of the EUC is obviously reduced, although the equatorial circulation remains qualitatively similar to the control run (Fig. 5c). The maximum speed is reduced to 50 cm s^{-1}, about a 25% reduction from the control run, although the wind is reduced by a half. This reflects the nonlinear nature of the EUC, as discussed in the appendix (A1). The reduced EUC intensity is also consistent with the weakened equatorial cell and the equatorial gyre as discussed before. The other obvious change is the thickness of the EUC; it reaches much less deep than in the control run. As a result, the transport of the EUC decreases by about a half as shown in Fig. 6 (curve c). Figure 5d shows that if the wind is reduced everywhere by a half, then the EUC is similar to that in Fig. 5c. It is interesting to notice that the small difference between Fig. 5d and Fig. 5c is similar to the small difference between Fig. 5b and Fig. 5a. In both pairs, a reduced subtropical wind curl even increases the maximum EUC speed slightly while it reduces the transport by about 1 Sv (Fig. 6), mainly because of a smaller width and thickness of the EUC.

According to Pedlosky's (1987, 1988) scaling argument, the dependence of EUC speed and transport on τ should be $\tau^{1/4}$ and $\tau^{7/8}$, respectively. The EUC speed should thus be less sensitive to the wind than the EUC transport, an implication qualitatively supported by our simulations. (Compare the standard run and the half-easterly run, or the half-tropical and the half-wind run.) Quantitatively, the dependence on τ of the GCM EUC transport is nearly linear, that is, close to $\tau^{7/8}$, while the dependence of the GCM EUC speed seems more linear than $\tau^{1/4}$. When the equatorial wind is reduced by a half, the maximum EUC speed is reduced about 25%, larger than the prediction of 12% from the 1/4 power. This is perhaps because Pedlosky's scaling argument assumes a pure inertial flow fed from the interior ocean. In the GCM, the EUC gains a substantial amount of water from the low-latitude western boundary current (Liu et al. 1994), where viscosity

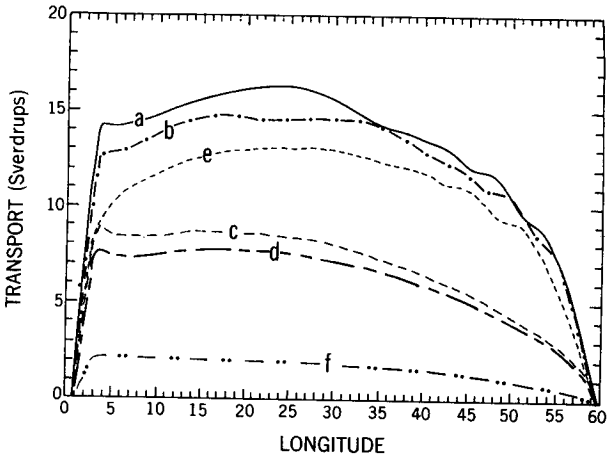

FIG. 6. The transport of the EUC (eastward transport within 5° latitude of the equator and in the upper 250 m) for each run: control run (curve a), half-subtropical run (curve b), half-easterly run (curve c), half-wind run (curve d), all-easterly run (curve e), and no-easterly run (curve f).

is strong. Thus, the velocity dependence on local wind becomes more linear in the GCM.

These four experiments confirm that the strength of the EUC is mainly determined by the tropical easterlies. The subtropical wind curl increases the EUC transport but only slightly. This notion is further supported by the two extreme runs. In the absence of a subtropical wind curl (Fig. 5e), a uniform easterly produces a well-developed EUC with a maximum speed (78 cm s^{-1}) larger than all the other runs. The thickness of the EUC is smaller than those in the runs with the same tropical easterly (control run and half-subtropical run), so that the transport is reduced by about 3 Sv (Fig. 6, curve e). When the local easterly is shut off, Figs. 5 and 6 (curve f) show that the EUC practically disappears, as does the subsurface eastward pressure gradient force along the equator (see later Fig. 7f).

The very weak EUC in Fig. 5f has an interesting yet subtle difference from the other cases: the EUC reaches its maximum speed at the western boundary in Fig. 5f but in the midbasin for other cases. This suggests that the EUC in Fig. 5f is forced by the mass from the subtropical gyre through the low-latitude western boundary current.[2] In other words, the subtropical curl influences

[2] As pointed out by one reviewer, this low-latitude western boundary current may also be related to the adjustment of the thermal field of the thermocline. This will be similar to the case of the deep western boundary current studied by Kawase (1987). Kelvin waves are excited by the adjustment caused by a source water in the polar region to form the deep western boundary current. This process is also possible in the thermocline if there is a source water in the poleward region. In this extreme case, the westward flow in the southern part of the subtropical gyre provides the source water. However, for more realistic wind forcings (as in other cases), it seems unlikely that the wind effect will be dominated by the buoyance effect at the depth of the thermocline.

the EUC mainly through the low-latitude western boundary current. This feature can indeed be identified in other cases. In Fig. 5a and Fig. 5c, in which the subtropical wind curl is strong, the EUC speed has a second maximum near the western boundary, which is close to the maximum in the midbasin (the difference is less than 10 cm s^{-1}). But, when the subtropical wind is reduced by a half (Fig. 5b and Fig. 5d), the second maximum of EUC speed near the western boundary is more than 10 cm s^{-1} less than the maximum EUC in the midbasin. In the extreme case without the subtropical wind curl, Fig. 5e shows that the second maximum almost disappears near the western boundary. This is shown even clearly in the transport of Fig. 6 (curve e). The all-easterly run has an EUC transport that increases more slowly from the western boundary toward the midbasin than in other runs. Hence, although the maximum transport and speed of the EUC is affected slightly by the subtropical wind curl, the zonal structure of EUC is determined to some extent by the subtropical wind. The subtropical wind curl tends to increase the EUC transport near the western boundary modestly.

Further observation of the EUC transport in Fig. 6 shows that, in the perturbation runs, the small reduction (about 1 Sv) of the EUC transport due to the half reduction of the subtropical wind is caused by the reduction of the initial EUC transport (compare curve b with curve a, and curve d with curve c). This is consistent with the above conclusion on the effect of the subtropical wind.

In short, the maximum EUC transport is mainly determined by the tropical easterly wind, because the easterly wind determines the subtropical–equatorial mass exchange. The subtropical wind influences the EUC slightly, mainly by changing the transport in the low-latitude western boundary current.

5. Equatorial thermocline under various winds

In contrast to the extensively studied subtropical thermocline, the dynamics of the equatorial thermocline has rarely been discussed. Figure 7 shows the temperature fields in the equatorial plane for the six runs. It is clear that the local easterly wind is crucial for the thermal field from the surface to below the thermocline. Compare Figs. 7a and 7c. When the tropical easterly is reduced by a half, the whole equatorial water column is warmed about 2°C almost uniformly down to 300 m. The higher temperature is clearly due to weaker upwelling. This feature is also true if one compares Fig. 7b with Fig. 7d. In the latter case, the temperature is about 2°C warmer than in the former. In the extreme case without local easterly winds, the thermocline becomes flat and is much warmer (Fig. 7f).

Figure 7 also shows that the subtropical wind is able to influence the lower part of the thermocline significantly. Compare the control run (Fig. 7a) with the half-subtropical run (Fig. 7b); the upper layer temperatures are almost identical. However, the temperature for the lower thermocline is higher by about 2°C for the stronger subtropical wind curl case in Fig. 7a. This suggests that a stronger subtropical wind will produce a warmer lower part of equatorial thermocline. This is also true if one compares the half-easterly run (Fig. 7c) with the half-wind run (Fig. 7d). The former has a stronger subtropical wind and a warmer lower equatorial thermocline, although the upper thermocline remains almost the same. This feature is also clear when the subtropical wind curl vanishes. The temperatures below the thermocline in the all-easterly run (Fig. 7e) are about 2°C and 4°C higher than the half-subtropical run (Fig. 7b) and the control run (Fig. 7a), respectively, although the temperature fields above the thermocline are almost identical in the three cases.

Since the subtropical wind only changes the lower part of equatorial thermocline, it can change the stratification of the equatorial thermocline significantly. A stronger subtropical wind warms the lower thermocline, creating a less stable stratification in the equatorial thermocline. With a strong subtropical wind curl, both the control run (Fig. 7a) and the half-easterly run (Fig. 7c) have a broad thermocline. In comparison, both the half-subtropical run (Fig. 7b) and the half-wind run (Fig. 7d) develop a narrow thermocline. If the subtropical wind curl vanishes, the thermocline is even sharper (Fig. 7e). If one calculates the maximum stratification ∂T_z in the western part of the equatorial ocean as the gradient between the 20° and 18°C isotherms, ∂T_z is about 1.3 to 1.5 times larger in Fig. 7b than in the control run (Fig. 7a). The maximum stratification of the all-easterly run (Fig. 7e) is more than twice that of the control run. The maximum stratification in the eastern ocean also has a similar tendency. Although the subtropical wind curl has little impact on the EUC transport, it has a significant impact on the equatorial thermocline. A reduction of the subtropical wind curl by a factor of 2 can increase the maximum stratification by 30% or so.

The change in temperature field affects the equatorial currents. The stronger stratification, due to a weaker subtropical wind, results in a smaller EUC depth and thickness, and shallower equatorial cell as seen in Figs. 3 and 5. This is because of a stronger thermal wind component. This is why, under a weaker subtropical wind, the maximum speeds of EUC become even slightly stronger, while the EUC transports decrease slightly.

The reason for the change in the equatorial thermocline when the subtropical winds change is evident in Fig. 8, which shows the meridional sections (in midbasin) of temperature. Under strong wind curl, the strong Ekman pumping produces a deeper subtropical thermocline and produces more mode water. This is seen by comparing Fig. 8a with Fig. 8b (or Fig. 8c with Fig. 8d); the former has a stronger wind curl and a

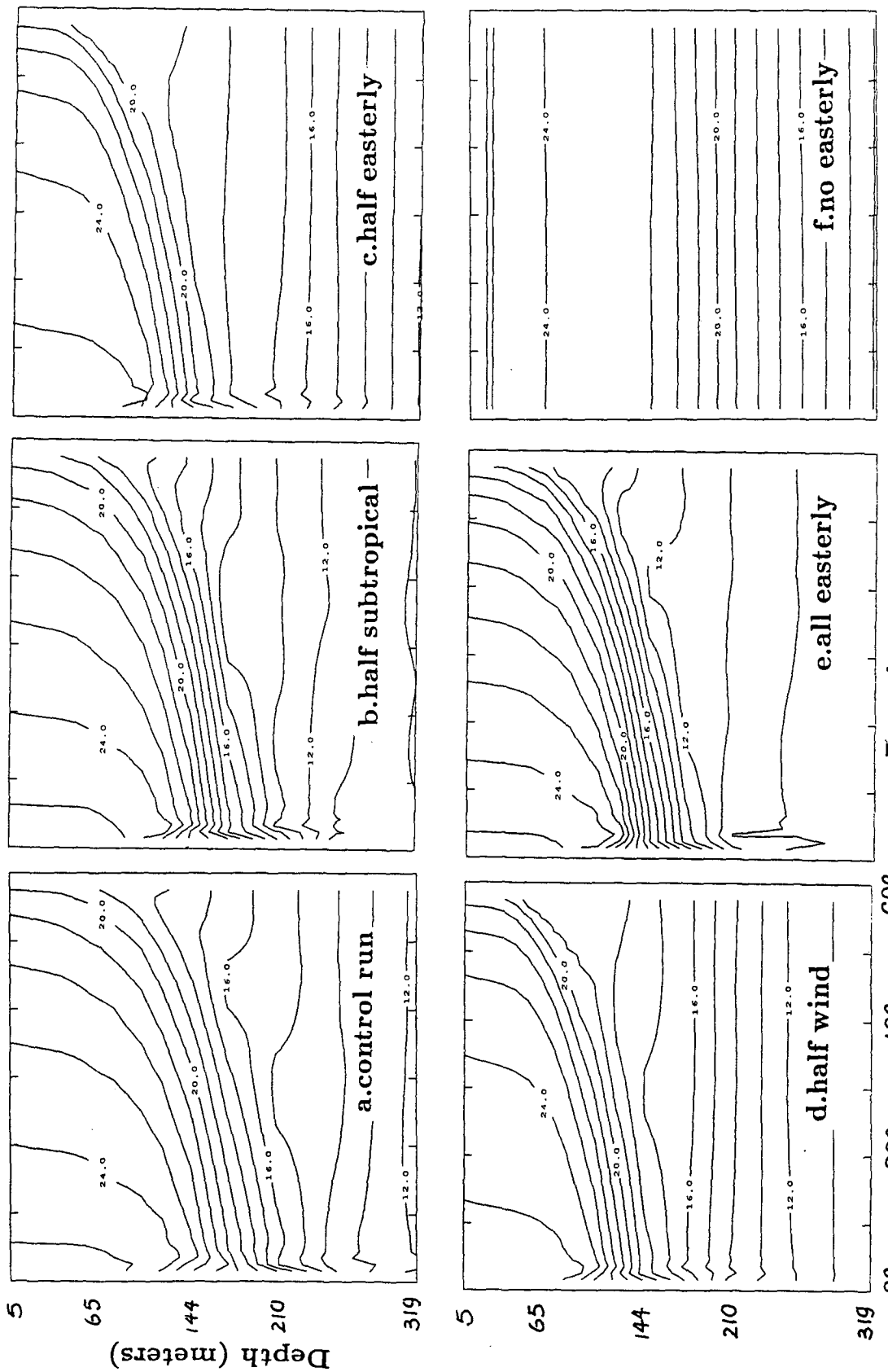

FIG. 7. Temperature field along the equatorial plane for (a) control run, (b) half-subtropical run, (c) half-easterly wind run, (d) half-wind run, (e) all-easterly run, and (f) no-easterly run. Contour interval: 1°C.

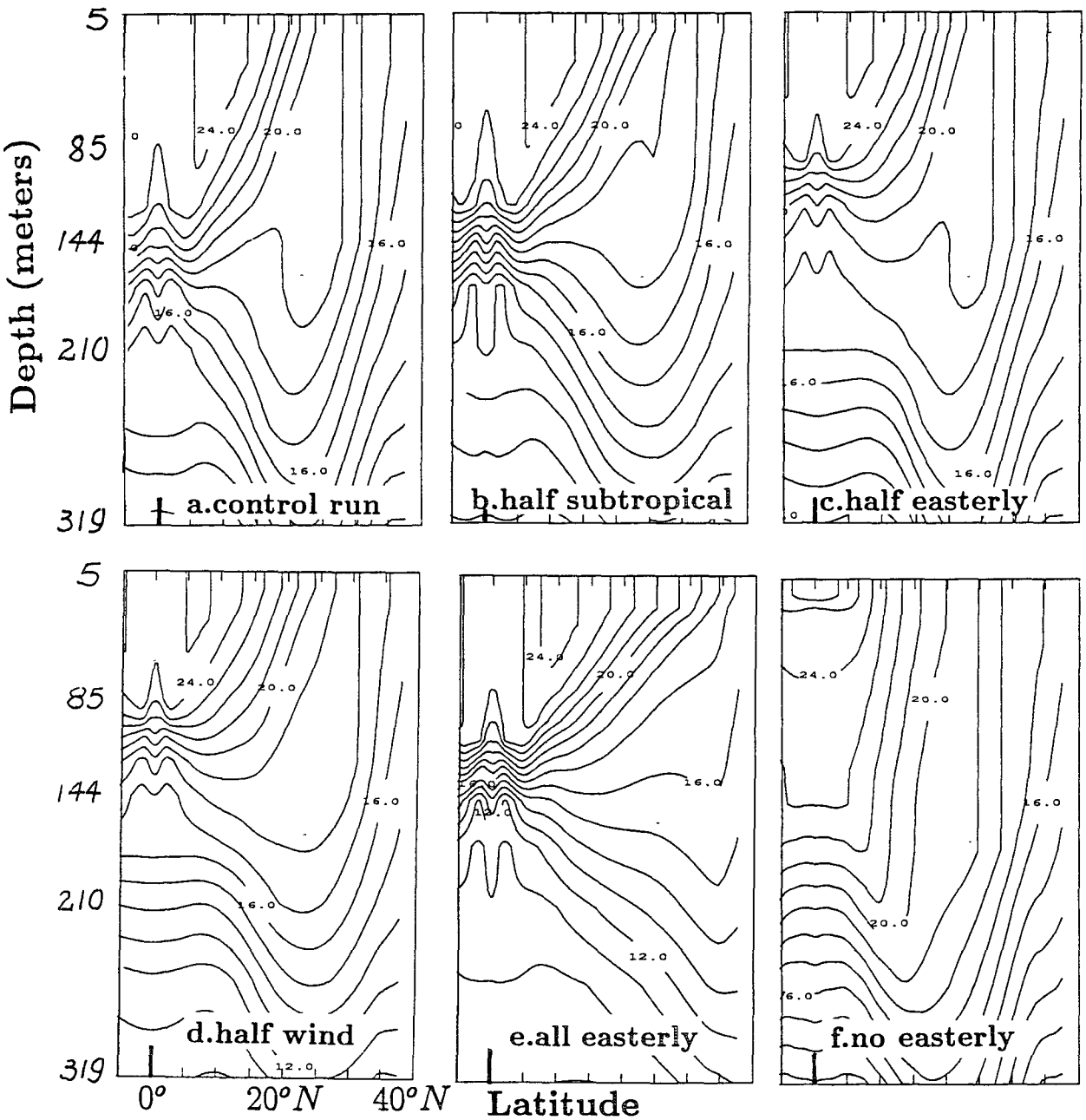

FIG. 8. Temperature field along the midbasin section for (a) control run, (b) half-subtropical wind run, (c) half-easterly run, (d) half-wind run, (e) all-easterly run, and (f) no-easterly run. Contour interval: 1°C.

deeper subtropical thermocline. Although the subtropical–equatorial mass exchange remains almost the same as can be seen in Figs. 4a,b (or Figs. 4c,d), the subsurface geostrophic flow advects warmer subtropical water equatorward, warming the deeper equatorial thermocline water. Thus, the temperature below 150 m is about 2°C warmer in the stronger subtropical wind curl case in Fig. 7a than in the weaker subtropical wind case in Fig. 7b (or warmer in Fig. 7c than in Fig. 7d).

One might expect that a stronger subtropical wind drives a stronger equatorward Sverdrup current and therefore transports more cold water to the equator. However, a stronger wind curl also increases the Ekman pumping–induced downwelling that causes warming. Thus, a stronger subtropical wind curl actually produces a stronger southward and downward detrainment mass flux, warming the subtropical and in turn the equatorial thermocline water. Hence, the equatorward

mass transport from the subtropics, although insignificant for the equatorial momentum balance, plays an important rule in the upper equatorial oceanic heat balance. This dominant advective balance nature of the thermocline field can be seen clearly in the term balance of the temperature equations in (A2) and (A3).

6. Concluding remarks

A set of GCM experiments demonstrates that the transport of the EUC is mainly determined by the easterly winds in the Tropics, although most of the EUC water comes from the subtropical gyre (Liu et al. 1994). With an increased subtropical wind (but fixed tropical easterly wind), the increased subtropical water simply recirculates within the subtropical gyre. The effect of the subtropical wind on the EUC transport is very limited ($\sim$1 Sv in the low-latitude western boundary current and therefore the initial EUC transport). However, the lower equatorial thermocline field is influenced strongly by the subtropical wind curl. A reduction of the subtropical wind curl causes colder waters to be transported to the subsurface equatorial region and cools the deeper part of equatorial thermocline. As a result, the stratification in the equatorial thermocline is intensified, and there is a tendency for the mean depth of the equatorial thermocline to become shallower.

The tropical winds affect the equatorial temperature field uniformly from the surface to below the thermocline. A stronger tropical wind intensifies the equatorial upwelling and lowers the temperature. However, the stratification in the thermocline is not affected. Since the thermal field will take a much longer time to reach the true equilibrium, we may expect some quantitative changes from our experiments. However, it seems unlikely that the conclusion about the equatorial thermocline will be changed qualitatively.

Further studies are needed to determine the factor that controls the mean depth and stratification of the equatorial thermocline. These factors control the prediction of the ENSO phenomena (since the prediction of the ENSO in some simple models depends crucially on the specified mean depth of the equatorial thermocline). A particularly unresolved feature of our model is the absence of a North Equatorial Countercurrent, which is bound to influence the links between the subtropics and equatorial zone. A further improvement to the model will be a change from the surface restoring temperature condition to a fixed heat flux condition. These experiments will be carried in the future.

Acknowledgments. We are indebted to Drs. J. Pedlosky, K. Bryan, R. Toggweiler, and S. Wacongne for numerous invaluable discussions and suggestions. R. Pacanowski and C. Koberle have been very patient in helping ZL with the GCM. One of us (ZL) was supported by the NOAA postdoctoral fellowship in climate change, and one (SGHP) was supported by the NOAA Grant NA26GP0057.

APPENDIX

Spinup of Tropical and Subtropical Temperature Field

The spinup of the equatorial currents has been studied in detail (e.g., by Philander and Pacanowski 1980), while the spinup of the subtropical thermocline has been investigated by Liu (1993) in a simple analytical model. The spinup of the temperature field near the equator, however, has rarely been discussed previously. We will briefly describe the evolution of the temperature equations in both the equatorial and subtropical regions.

The spinup of the equatorial current mainly involves the initial downward and eastward propagation Kelvin wave and the upward and westward Rossby wave. The EUC is established in about a month after the Kelvin wave passes the basin. The final balance in a central basin equatorial subsurface box (25°–35°, 2°S–2°N, 100–232 m) is dominated by

$$uu_x + vu_y + wu_z - fv = -p_x > 0. \qquad \text{(A1)}$$

This balance is the inertial balance proposed by Pedlosky (1987).

The evolution for the equatorial subsurface temperature equation is presented in Fig. A1a. Initially, the upwelling (curve D) cools the temperature. After about 2 months, by building up the EUC, the arrival of the Kelvin wave produces a strong warm advection from the west (curve B). The cooling of temperature is then stopped, although upwelling still exhibits a high-frequency oscillation. After about two years, the local variability (curve A) vanishes and a quasi-equilibrium is achieved such that the upwelling is balanced by the warm zonal advection, and to a lesser extent by the meridional convergence of warm subsurface water; that is,

$$uT_x + vT_y + wT_z = 0. \qquad \text{(A2)}$$

It is important to note that in the subsurface both momentum and temperature equations [(A1) and (A2)] are dominated by advection. The dominance of advection in the temperature equation implies a weak entrainment. Calculations show that the entrainment velocity along the equator is one order smaller than the upwelling velocity (not shown), consistent with observations (Bryden and Brady 1985). Near the surface, the momentum transfer and heat transfer become important in the zonal momentum and temperature equations, while nonlinear advection becomes weaker. The analysis of the momentum equation (A1) is consistent with Wacongne's (1989, 1990) analysis of the GCM results of the Atlantic.

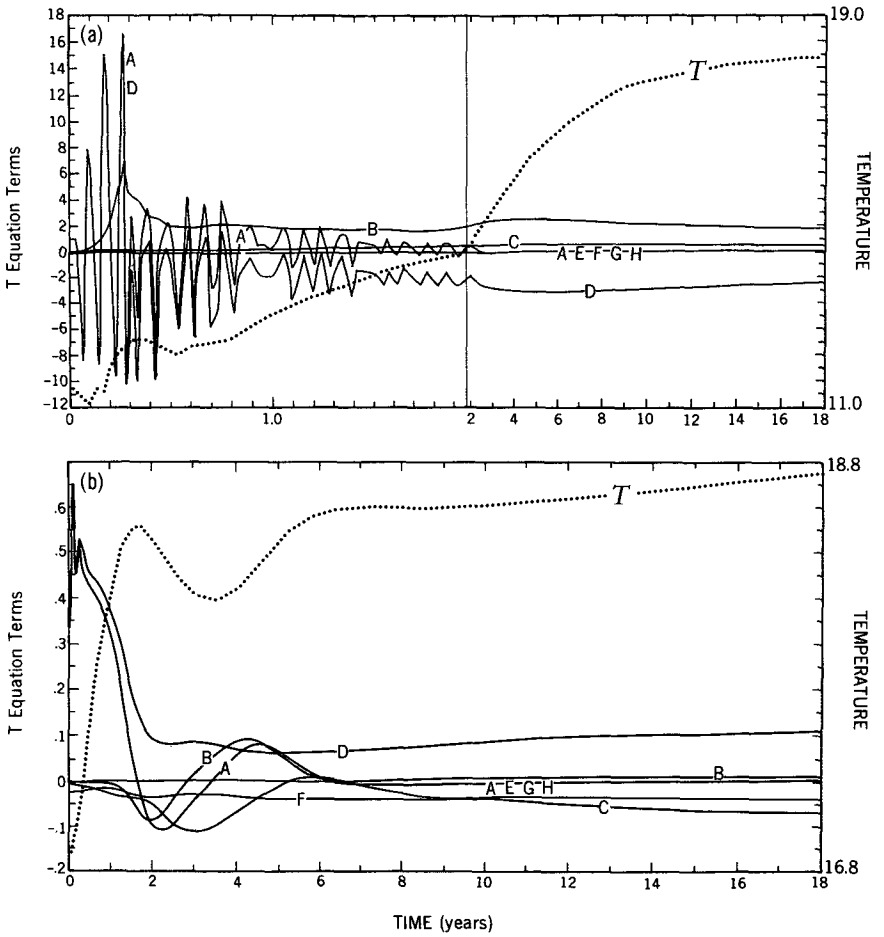

FIG. A1. The evolution of terms (in units of 10^{-7} °C s^{-1}) for the temperature equations in the two boxes confined in the central basin subsurface thermocline (25°–35°, 100–232 m) (a) on the equator (2°S, 2°N), and (b) the subtropical gyre 29°S–19°S. The labeled curves correspond to terms: A:T_t, B: $-uT_x$, C: $-vT_y$, D: $-wT_z$, E:k_hT_{xx}, F:k_hT_{yy}, G:$(k_vT_z)_z$, H: *heating source term*. Here k_h and k_v are the horizontal and vertical diffusivities. The heavy dotted curve is the temperature.

The evolution of momentum equations in the subtropics is simply geostrophic balance in the subsurface and Ekman drift on the surface. Now, the velocity components adjust to the pressure gradient, which varies slowly with the temperature field.

The evolution of the subsurface temperature field is shown in Fig. A1b. Now the vertical velocity is downward due to Ekman pumping, which yields a downwelling warming. The evolution is much slower than the equatorial region because of both the slow Rossby wave and currents in the extratropics. Initially, a strong warming (curve D) is produced by the local Ekman downwelling. After one year, the downwelling warming is reduced dramatically while the southward cold advection (curve C) increases significantly. This is caused by the arrival of subducted water. Indeed, as can be seen from the momentum equations (not shown), the ventilation water suppresses the downwelling but increases the southward current significantly. After 6 years the local variability becomes negligible. A quasi-equilibrium is established between the warm downwelling and southward cold advection. The meridional diffusion also seems to play a secondary role, which is probably exaggerated by the coarse resolution in the midlatitudes. The final balance is, thus,

$$vT_y + wT_z = (K_hT_y)_y, \qquad \text{(A3)}$$

where K_h is the horizontal diffusivity. This spinup process of a ventilated thermocline is similar to that discussed in a simple thermocline model (Liu 1993). The dominant advection effect is similar to the equatorial thermocline in (A2). To the east of the shadow zone, the meridional advection is likely to be weak. Downwelling warming tends to be balanced by diffusion.

Near the surface, the heat flux becomes important too.

REFERENCES

Bryan, K., 1969: A numerical method for the study of the circulation of the world ocean. *J. Comput. Phys.*, **4,** 347–376.

Bryden, L. H., and E. C. Brady, 1985: Diagnostic model of the three-dimensional circulation of the upper equatorial Pacific Ocean. *J. Phys. Oceanogr.*, **15,** 1255–1273.

Fine, R. A., 1987: The penetration of tritium into the tropical Pacific. *J. Phys. Oceanogr.*, **17,** 553–564.

——, J. L. Reid, and H. G. Ostlund, 1981: Circulation of tritium in the Pacific Ocean. *J. Phys. Oceanogr.*, **11,** 3–14.

Kawase, M., 1987: Establishment of deep ocean circulation driven by deep water formation. *J. Phys. Oceanogr.*, **17,** 2294–2316.

Liu, Z., 1993: Thermocline forced by varying wind. Part I: Spin-up and spin-down. *J. Phys. Oceanogr.*, **23,** 2505–2522.

——, 1994: A simple model of the mass exchange between the subtropical and tropical ocean. *J. Phys. Oceanogr.*, **24,** 1153–1165.

——, S. G. H. Philander, R. C. Pacanowski, 1994: A GCM study of subtropical–tropical upper-ocean water exchange. *J. Phys. Oceanogr.*, **24,** 2606–2623.

McCreary, J., and Z. Yu, 1992: Equatorial dynamics in a $2\frac{1}{2}$-layer model. *Progress in Oceanography,* Vol. 29, Pergamon, 61–132.

——, and P. Lu, 1994: Interaction between the subtropical and equatorial ocean circulations: The subtropical cell. *J. Phys. Oceanogr.*, **24,** 466–497.

Pacanowski, R. C., and S. G. H. Philander, 1981: Parameterization of vertical mixing in numerical models of tropical oceans. *J. Phys. Oceanogr.*, **11,** 1443–1451.

——, K. W. Dixon, and A. Rosati, 1991: The GFDL Modular Ocean Model Users Guide. GFDL Ocean Group Tech. Rep. No. 2.

Pedlosky, J., 1987: An inertial theory of the equatorial undercurrent. *J. Phys. Oceanogr.*, **17,** 1978–1985.

——, 1988: Entrainment and the termination of the Equatorial Undercurrent. *J. Phys. Oceanogr.*, **18,** 880–886.

Philander, S. G. H., and R. C. Pacanowski, 1980: The generation of equatorial currents. *J. Geophys. Res.*, **85,** 1123–1136.

Tsuchiya, M., 1981: The origin of the Pacific 13°C water. *J. Phys. Oceanogr.*, **11,** 794–812.

——, R. Lukas, R. A. Fine, E. Firing, and E. Lindstorm, 1989: Source waters of the Pacific Equatorial Undercurrent. *Progress in Oceanography,* Vol. 23, Pergamon, 101–147.

Toggweiler, R., K. Dixon, and W. S. Broecker, 1989: The Peru upwelling and the ventilation of the South Pacific thermocline. *J. Geophys. Res.*, **96,** 20 467–20 497.

Wacongne, S., 1989: Dynamical regimes of a fully nonlinear stratified model of the Atlantic Equatorial Undercurrent. *J. Geophys. Res.*, **94**(C4), 4801–4815.

——, 1990: On the difference in strength between Atlantic and Pacific undercurrents. *J. Phys. Oceanogr.*, **20,** 792–799.